Available online at www.sciencedirect.com
SCIENCE DIRECT®
Journal of Molecular Structure 693 (2004) 103–118
Journal of MOLECULAR STRUCTURE
www.elsevier.com/locate/molstruc

Conformational analysis of a trihydroxylated derivative of cinnamic acid—a combined Raman spectroscopy and Ab initio study

S.M. Fiuza[a], E. Van Besien[a,b], N. Milhazes[c,d], F. Borges[c], M.P.M. Marques[a,e,*]

[a]*Unidade I and D 'Química-Física Molecular', Faculdade de Ciências e Tecnologia, Universidade de Coimbra, 3000 Coimbra, Portugal*
[b]*Dept. Chemie, Katholieke Univ Leuven, 3001 Heverlee, Belgium*
[c]*Química Orgânica, Fac. Farmácia, Univ Porto, 4050-047 Porto, Portugal*
[d]*Institute Sup. Ciências Saúde-Norte, 4580 Paredes, Portugal*
[e]*Dept. Bioquímica, Faculdade de Ciências e Tecnologia, Univ. Coimbra, Ap. 3126, 3001-401 Coimbra, Portugal*

Received 8 January 2004; revised 2 February 2004; accepted 2 February 2004

Abstract

A conformational analysis of 3-(3,4,5-trihydroxyphenyl)-2-propenoic acid (3,4,5-trihydroxycinnamic acid, THPPE), a trihydroxylated cinnamic acid analogous to caffeic acid (a natural compound often present in diet), was carried out by Raman spectroscopy coupled to Ab initio MO calculations. Apart from the optimised geometrical parameters for the most stable conformers of this compound, and for one of its dimeric species, the corresponding harmonic vibrational frequencies, as well as potential-energy profiles for rotation around several bonds within the molecule, were obtained. Twenty one distinct conformers were found for THPPE, the lowest energy ones—THPPE 1 and THPPE 2—displaying a completely planar geometry. The conformational preferences of this system were thus found to be mainly ruled by the stabilising effect of π-electron delocalisation. At the light of these results, a complete assignment of the corresponding solid state Raman spectra was performed.

Keywords: Hydroxycinnamic acid derivatives; Raman spectroscopy; Ab initio calculations; Conformational analysis

1. Introduction

Phenolic acid derivatives constitute a group of natural compounds present in human diet in significative amounts, which have long been known to display both antioxidant (through their radical scavenging activity) and prooxidant properties [1–3]. They are involved in numerous metabolic reactions and are naturally occurring in many plant-derived food products, were they are largely responsible for the browning process [4–6]. Apart from being widely used as antioxidant food additives [7,8], some of them were lately found to behave as inhibitors of deleterious oxidative processes—e.g. in the prevention of cardiovascular diseases and inflammatory processes [9,10], or even in cancer [11–17]. Consequently, in the last few years there has been a growing interest in the understanding of the mechanisms associated to the biochemical role of phenolic compounds, which, in turn, was found to be strongly dependent on their structural characteristics [2,18,19].

The knowledge of the conformational preferences of this type of compounds is thus of the utmost importance as a starting point for future studies aiming at the understanding of the structure–activity relationships underlying their biological activity, which may contribute to the wider goal of developing new and more effective therapeutic agents (e.g. anticancer drugs). Nevertheless, the reported Ab initio molecular orbital calculations on phenolic acid derivatives are very scarce [20–25], semiempirical quantum-chemical methods being commonly used instead. Moreover, even these studies have aimed exclusively at the explanation of the structural dependency of the antioxidant activity of these phenols (e.g. caffeic acid [24]), focusing only on their most stable geometries.

In the present study, a complete conformational analysis of 3-(3,4,5-trihydroxyphenyl)-2-propenoic acid (3,4,5-trihydroxycinnamic acid, THPPE) − which is the trihydroxylated analogue to *trans*-caffeic acid − was carried out, by

* Corresponding author. Tel.: +351-239-853-600; fax: +351-239-853-607.
E-mail address: pmc@ci.uc.pt (M.P.M. Marques).

0022-2860/$ - see front matter © 2004 Elsevier B.V. All rights reserved.
doi:10.1016/j.molstruc.2004.02.019

both Raman spectroscopy and Ab initio MO calculations. Both the corresponding ethyl ester − ethyl 3-(3,4,5-trihydroxyphenyl)-2-propenoate (ethyl 3,4,5-trihydroxycinnamate, ETHPPE) − and *trans*-caffeic acid were studied for comparison purposes (namely aiming at a thorough spectral assignment).

2. Experimental

2.1. Synthesis

3-(3,4,5-trihydroxyphenyl)-2-propenoic acid (3,4,5-trihydroxycinnamic acid, THPPE) and ethyl 3-(3,4,5-trihydroxyphenyl)-2-propenoate (ethyl 3,4,5-trihydroxycinnamate, ETHPPE). A suspension of 3,4,5-trihydroxybenzaldehyde (1.0 g), malonic acid (1.0 g) or mono-ethylmalonate (1.2 g), anhydrous pyridine (5 ml) and four drops of aniline was stirred overnight, at 50 °C. After cooling, ethyl ether was added (50 ml). The organic phase was washed with HCl-2N and water, and dried over Na_2SO_4. The solvent was then evaporated and the residue was recrystallized from ethyl ether to yield the pretended compounds as light yellow solids.

3,4,5-Trihydroxycinnamic acid (THPPE). Yield 35%; FTIR $\upsilon_{max.}$ (cm^{-1}): 3510, 3382, 1666, 1618, 1597, 1539, 1454, 1425, 1388, 1317, 1221, 1151, 1028, 980, 914, 831, 800, 721, 634, 596, 542, 484. ^{1}H-NMR δ: 6.09 (1H, *d*, J = 15.8, H(α)),6.57 (2H, *s*, H(2), H(6)), 7.32 (1H, *d*, J = 15.8, H(β)), 8.74 (1H, *s*, O*H*), 9.17 (2H, *s*, O*H*); ^{13}C-NMR δ: 107.5 C(2, 6), *115.2*C(α), 124.6 C(1), 136.3 C(4), *145.1* C(β), *146.2* C(3, 5), 168.0 (C=O); EI-MS *m/z* (%): 196 ($M^{+\cdot}$, 100), 179 (22); 152 (57), 133 (27), 105 (16), 78 (51), 63 (57); mp 186–188 °C.

Ethyl 3,4,5-trihydroxycinnamate (ETHPPE). Yield 65%; FTIR $\upsilon_{max.}$ (cm^{-1}): 3394, 1656, 1601, 1508, 1467, 1371, 1317, 1277, 1203, 1142, 1034, 976, 845, 634, 596, 594. ^{1}H-NMR δ: 1.23 (3H, *s*, C*H*$_3$),.4.15 (2H, *q*, C*H*$_2$), 6.18 (1H, *d*, J = 15.8, H(α)),6.60 (2H, *s*, H(2), H(6)), 7.38 (1H, *d*, J = 15.8, H(β)), 8.80 (1H, *s*, O*H*), 9.18 (2H, *s*, O*H*); ^{13}C-NMR δ: *14.4* (CH_3), *59.8* (CH_2), *107.7* C(2, 6), *114.2* C(α), 124.5 C(1), 136.5 C(4), *145.5* C(β), 146.2 C(3, 5), 166.6 (C=O); EI-MS *m/z* (%): 224 ($M^{+\cdot}$, 100), 196 (17); 179 (86), 152 (48), 133 (40), 105 (21), 77 (32); mp 176–179 °C.

Apparatus. Infrared spectra were recorded on an ATI Mattson Genesis Series FTIR spectrophotometer using potassium bromide disks; only the most significant absorption bands are reported ($\upsilon_{max.}$, cm^{-1}). ^{1}H and ^{13}C NMR data were acquired, at room temperature, on a Brüker AMX 300 spectrometer, operating at 300.13 and 75.47 MHz, respectively. Dimethylsulfoxide-d_6 was used as a solvent; chemical shifts are expressed in δ (ppm), relative to tetramethylsilane (TMS) which was used as an internal reference; coupling constants (J) are given in Hz. Assignments were also made from DEPT (underlined values). Electron impact mass spectra (EI-MS) were carried out on a VG AutoSpec instrument; the data are reported as *m/z* (% of relative intensity of the most important fragments). Melting points were obtained on a Köfler microscope (Reichert Thermovar) and are uncorrected.

Other conditions. Thin-layer chromatography (TLC) was carried out on precoated silica gel 60 F254, with a layer thickness of 0.2 mm. The following systems were used for analytical control: silica gel, ethyl ether and chloroform/acetone (6:4). The spots were visualised under UV detection (254 and 366 nm), iodine vapour and $FeCl_3$ (5%).

2.2. Ab initio MO calculations

The Ab initio calculations − full geometry optimisation and calculation of the harmonic vibrational frequencies − were performed using the GAUSSIAN 98W program [26], within the Density Functional Theory (DFT) approach, in order to properly account for the electron correlation effects (particularly important in this kind of conjugated systems). The widely employed hybrid method denoted by B3LYP [27–32], which includes a mixture of HF and DFT exchange terms and the gradient-corrected correlation functional of Lee, Yang and Parr [33,34], as proposed and parametrised by Becke [35,36], was used, along with the double-zeta split valence basis sets 6-31G* and 6-31G** [37,38].

Molecular geometries (of both monomeric and dimeric species) were fully optimised by the Berny algorithm, using redundant internal coordinates [39]: The bond lengths to within ca. 0.1 ppm and the bond angles to within ca. 0.1°. The final root-mean-square (rms) gradients were always less than 3×10^{-4} hartree.bohr^{-1} or hartree.radian^{-1}. No geometrical constraints were imposed on the molecules under study. The 6-31G** basis set was used for all geometry optimisations, while for most of the rotational energy barrier calculations the smaller basis 6-31G* was found to yield good results. All frequency calculations were run at the B3LYP/6-31G** level and wavenumbers above 400 cm^{-1} were scaled [40] before comparing them with the experimental data. The basis set superposition error (BSSE) correction for the dimerisation energies was estimated by counterpoise (CP) calculations.

Quantitative potential-energy profiles for rotation around different bonds within the molecule were obtained, by scanning the corresponding dihedrals and using least-squares fitted Fourier-type functions of a dihedral angle, τ [41,42]:

$$P = \sum_{n=1}^{3} \frac{1}{2} P_n [1 - \cos(n\tau)] + \sum_{m=1}^{2} \frac{1}{2} P'_m \sin(m\tau) \quad (1)$$

The parameters P_n and P'_m correspond to potential-energy (V_n and V_m terms), bond-distance or bond-angle differences relative to a reference value. According to the symmetry of the molecule under study, the sine terms, which are of

significance only for asymmetric functions around 180°, were not included in the fitting of the experimental data.

2.3. Raman spectroscopy

The Raman spectra were obtained at room temperature, in a triple monochromator Jobin–Yvon T64000 Raman system (0.640 m, *f*/7.5) with holographic gratings of 1800 grooves.mm^{-1}. The detection system was a non-intensified CCD (Charge Coupled Device) and the entrance slit was set to 200 μm. The 514.5 nm line of an Ar^+ laser (Coherent, model Innova 300) was used as excitation radiation, providing ca. 70 mW at the sample position. Samples were sealed in Kimax glass capillary tubes of 0.8 mm inner diameter. Under the above mentioned conditions, the error in wavenumbers was estimated to be within 1 cm^{-1}. Spectra were collected both for solid samples and for DMSO-d_6 solutions (40 mM).

Fourier transform Raman spectra were recorded on a RFS 100/S Bruker spectrometer, with a 180° geometry, equipped with an InGaAs detector. Near-infrared excitation was provided by the 1064 nm line of a Nd:YAG laser (Coherent, model Compass-1064/500 N). A laser power of 200 mW at the sample position was used in all cases, and resolution was set to 2 cm^{-1}.

2.4. Reagents

3,4,5-trihydroxyaldehyde, *trans*-caffeic acid, mono-ethylmalonate and malonic acid were purchased from Sigma-Aldrich Química S. A. (Sintra, Portugal). Dimethyl-sulfoxide-d_6 (99.8%) was obtained from E. Merck, Darm-stadt, Germany. All other reagents and solvents were pro analysis grade, purchased from Merck (Lisbon, Portugal).

3. Results and discussion

3.1. Ab initio MO calculations

The geometries and relative energies of the distinct conformers of 3-(3,4,5-trihydro-xyphenyl)-2-propenoic acid (THPPE) were obtained, through Ab initio MO calculations (Fig. 1). The effect of several structural parameters on the overall stability of this molecule was investigated, namely: (i) S-*cis* or S-*trans* conformation of the carboxylic group-($H_{21}O_{13}C_{11}O_{12}$) equal to 0° or 180°, respectively (atoms numbered according to Fig. 1); (ii) orientation of the three phenolic hydroxyls (relative to the ring) − dihedrals ($H_{22}O_{14}C_1C_2$), ($H_{18}O_7C_6C_1$) and ($H_{17}O_8C_5C_6$) equal to 0° or 180°; (iii) relative orientation of the aromatic ring and the carboxylic moiety—($O_{12}C_{11}C_{10}C_9$) equal to 0° or 180°, and ($C_{11}C_{10}C_9C_3$) equal to 180° or 0°, the former defining a *trans* or *cis* orientation, respectively, of the ring relative to the carboxylate (around the linear chain C=C bond). Rotational isomerism was also investigated for this molecule, by scanning particular dihedral angles, in view of determining the corresponding rotational energy barriers—e.g. ($O_{12}C_{11}C_{10}C_9$) and ($C_4C_3C_9H_{19}$), which define the internal rotation of the carboxylic group and the aromatic ring, respectively (Fig. 1).

Twenty one different conformers were found (Fig. 1), the most stable ones displaying an S-*cis* orientation of the terminal carboxylic group. Except for THPPE 5 ($\Delta E = 10.9$ kJ mol^{-1}, out-of-plane H_{18}–($H_{18}O_7C_6C_5$) = 91.7°), THPPE 17 ($\Delta E = 31.1$ kJ mol^{-1}, out-of-plane H_{18}–($H_{18}O_7C_6C_5$) = 89.7°), THPPE 21 ($\Delta E = 37.2$ kJ mol^{-1}, out-of-plane H_{18}–($H_{18}O_7C_6C_5$) = 91.5°) and THPPE 18 ($\Delta E = 33.2$ kJ mol^{-1}, out-of-plane H_{21}–($H_{21}O_{13}C_{11}C_{10}$) = 12.7°), all other energy minima have a planar geometry (C_s symmetry), probably due to the stabilising effect of π-electron delocalisation between the ring and the C_9=C_{10} and C_{11}=O_{12} double bonds, which is favoured when they are coplanar. In fact, the four most stable conformers found-THPPE 1 to THPPE 4—are completely planar ones (Fig. 2). Actually, THPPE 5, which displays a quasi-perpendicular orientation of the -O_7H_{18} group (($H_{18}O_7C_6C_5$) = 91.7°), has a much higher relative energy ($\Delta E = 10.9$ kJ mol^{-1}, Fig. 1).

The conformational characteristics of THPPE were also determined to be highly dependent on the geometry of the carboxylic group − either S-*cis* or S-*trans*—the former being strongly favoured: THPPE 1 (ΔE = 0) vs THPPE 12 ($\Delta E = 25.5$ kJ mol^{-1}), THPPE 2 ($\Delta E = 0.5$ kJ mol^{-1}) vs THPPE 13 ($\Delta E = 28.0$ kJ mol^{-1}), THPPE 5 ($\Delta E = 10.9$ kJ mol^{-1}) vs THPPE 21 ($\Delta E = 37.2$ kJ mol^{-1}), or THPPE 6 ($\Delta E = 11.5$ kJ mol^{-1}) vs THPPE 19 (ΔE = 36.3 kJ mol^{-1}) (Figs. 1 and 2). Moreover, it was verified that the orientation of the ring hydroxyl groups has an influence on the conformation of the carbon pendant chain. In fact, the geometry corresponding to an identical orientation of these groups is energetically favoured, once it minimises steric repulsions between adjacent OH's, and allows the formation of medium strength intramolecular $H_{17}\cdots O_7$ and $H_{18}\cdots O_{14}$, or $H_{22}\cdots O_7$ and $H_{18}\cdots O_8$ bonds (O···H distances between 217 and 219 pm, for the most stable conformers, Fig. 1). As expected, only high energy geometries (ΔE ≥ 16 kJ mol^{-1}) were obtained when any two ring hydroxyls were directed towards each other: THPPE 7, THPPE 8, THPPE 9, THPPE 10, THPPE 14 and THPPE 15—displaying an $O_{14}\cdots O_7$ distance of ca. 269 pm-and THPPE 20-with a $H_{18}\cdots H_{17}$ distance of 196 pm (Fig. 2). As to the relative orientation of the terminal carboxylic group relative to the phenolic hydroxyls, THPPE behaves differently from its analogue caffeic acid (CA) [25], due to the presence of a third OH ring substituent, which is responsible for a higher symmetry of the molecule. Thus, as opposed to CA, a *syn* conformation (i.e. with C=O and ring OH's pointing to the same side relative to the carbon chain) is preferred over an *anti* one, either for a ($C_{10}C_9C_3C_2$) dihedral equal to 180° − THPPE 1 ($\Delta E = 0$ kJ mol^{-1}) vs THPPE 2

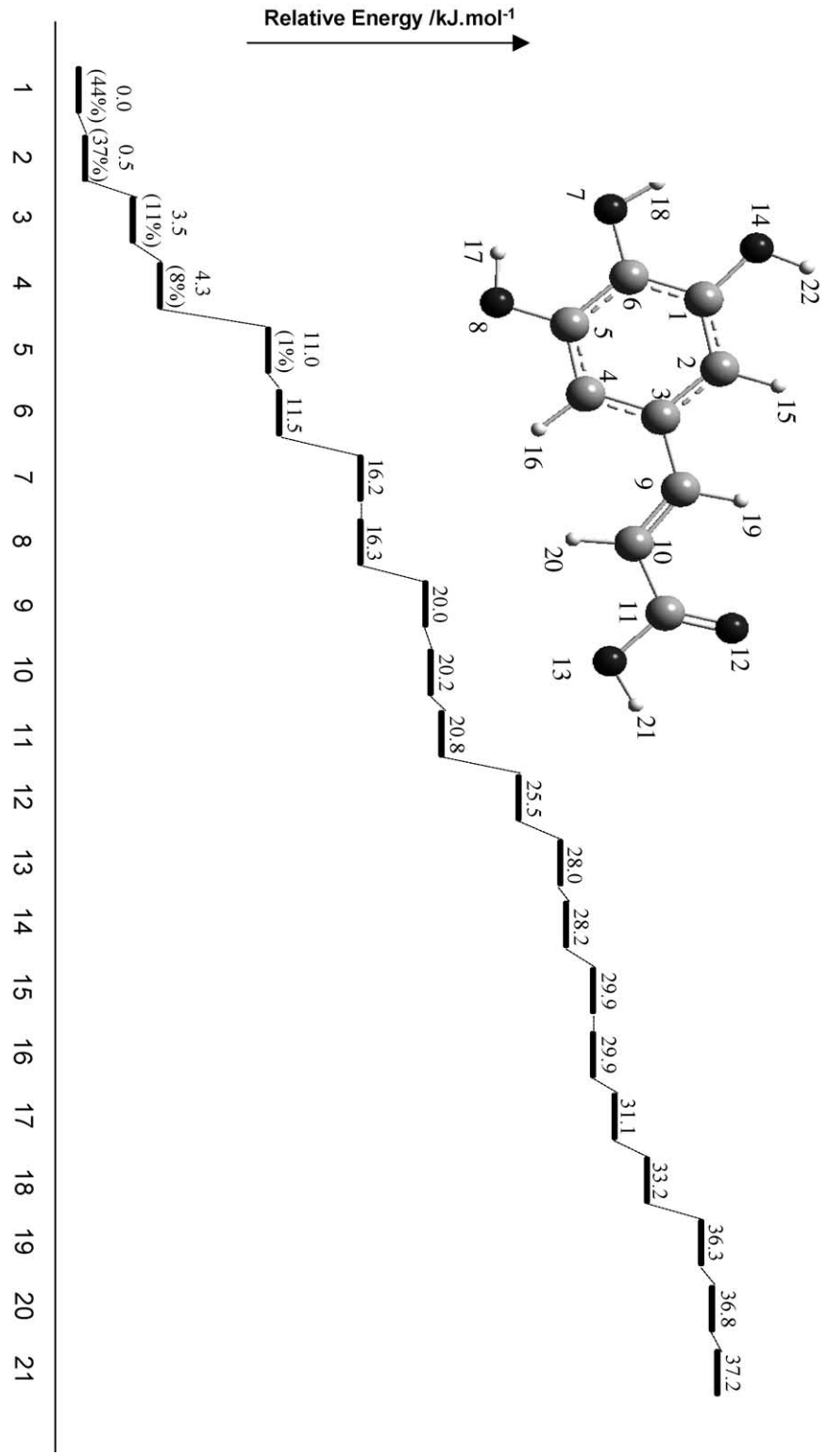

Fig. 1. Schematic representation of the calculated (B3LYP/6-31G**) conformational energies (and populations, at 25 °C) for 3-(3,4,5-trihydroxyphenyl)-2-propenoic acid (THPPE). (The atom numbering is included).

($\Delta E = 0.5$ kJ mol^{-1})/THPPE 4 ($\Delta E = 4.3$ kJ mol^{-1}), and THPPE 12 ($\Delta E = 25.5$ kJ mol^{-1}) vs THPPE 13 ($\Delta E = 36.3$ kJ mol^{-1})—or 0°—THPPE 3 ($\Delta E = 3.5$ kJ mol^{-1}) vs THPPE 4 ($\Delta E = 4.3$ kJ mol^{-1}), and THPPE 6 ($\Delta E = 11.5$ kJ mol^{-1}) vs THPPE 11 ($\Delta E = 20.8$kJ mol^{-1}) (Fig. 2).

Consideration of a *cis* orientation of the ring and the carboxylate group relative to the C_9=C_{10} bond − ($C_{11}C_{10}C_9C_3$)

and ($C_{10}C_9C_3C_2$) equal to 0° − led to rather high energy conformers: THPPE 6 ($\Delta E = 11.5$ kJ mol^{-1}), THPPE 11 ($\Delta E = 20.8$ kJ mol^{-1}), THPPE 14 ($\Delta E = 28.2$ kJ mol^{-1}), THPPE 15 ($\Delta E = 29.9$ kJ mol^{-1}), THPPE 16 ($\Delta E = 29.9$ kJ mol^{-1}), THPPE 17 ($\Delta E = 31.1$ kJ mol^{-1}) and THPPE 19 ($\Delta E = 36.3$ kJ mol^{-1}). Actually, despite the possibility of occurrence of O···H intramolecular interactions, yielding a seven-membered intramolecular ring (Fig. 2), these geometries are not stabilised over the ones displaying a linear carbon chain, for which π-delocalisation is surely more effective. THPPE 6 is significantly stabilised as compared to the other similar conformations, through the occurrence of a rather strong $O_1\cdots{}_2H_{15}$ interaction (($O_{12}\cdots H_{15}$) = 201 pm) coupled to a planar geometry displaying

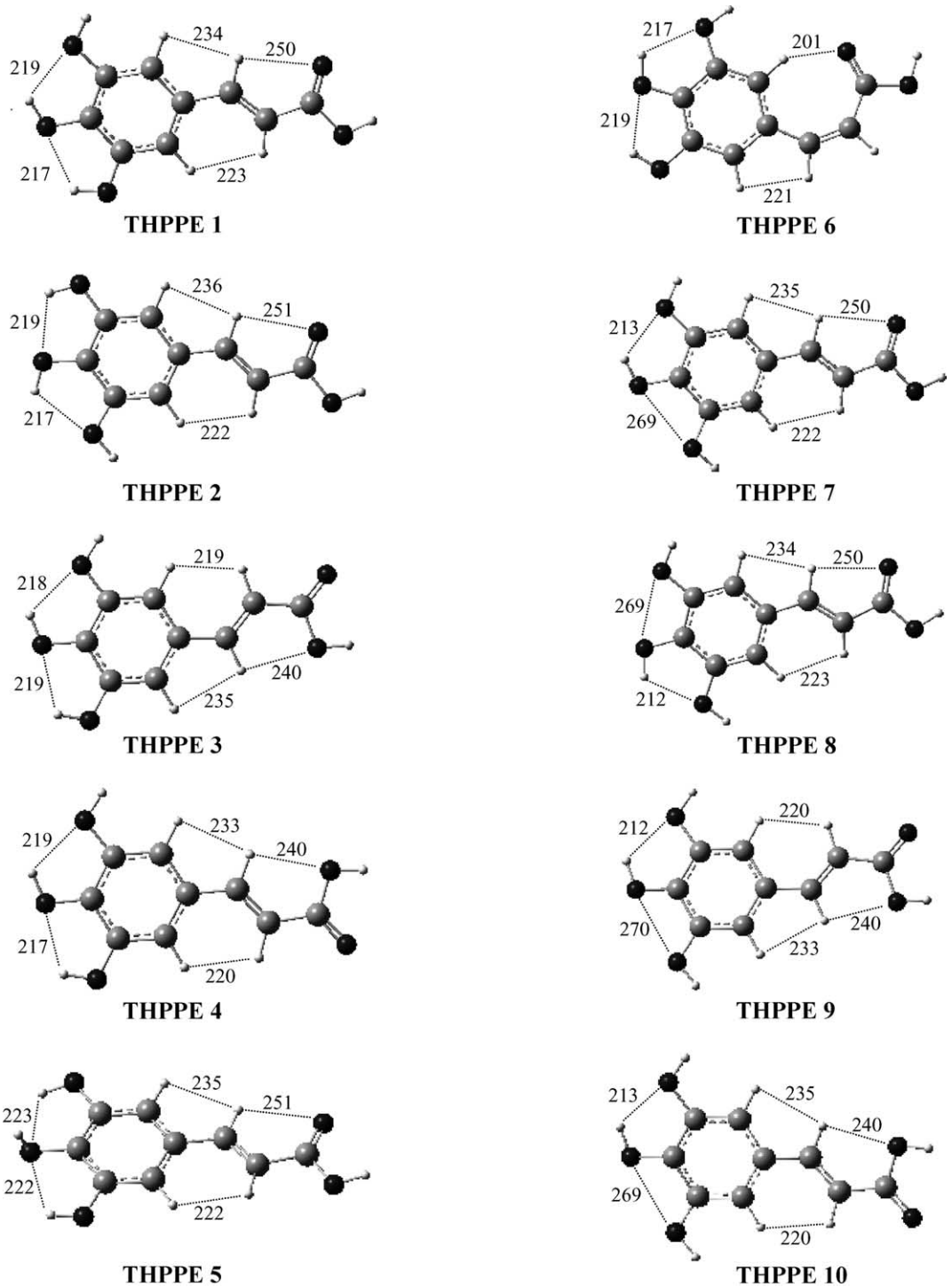

Fig. 2. Representation of the several conformers calculated for 3-(3,4,5-trihydroxy phenyl)-2-propenoic acid (THPPE) − displaying (C)H···O and (O)H···O intramolecular interactions. (B3LYP/6-31G** level of calculation. Distances are represented in pm).

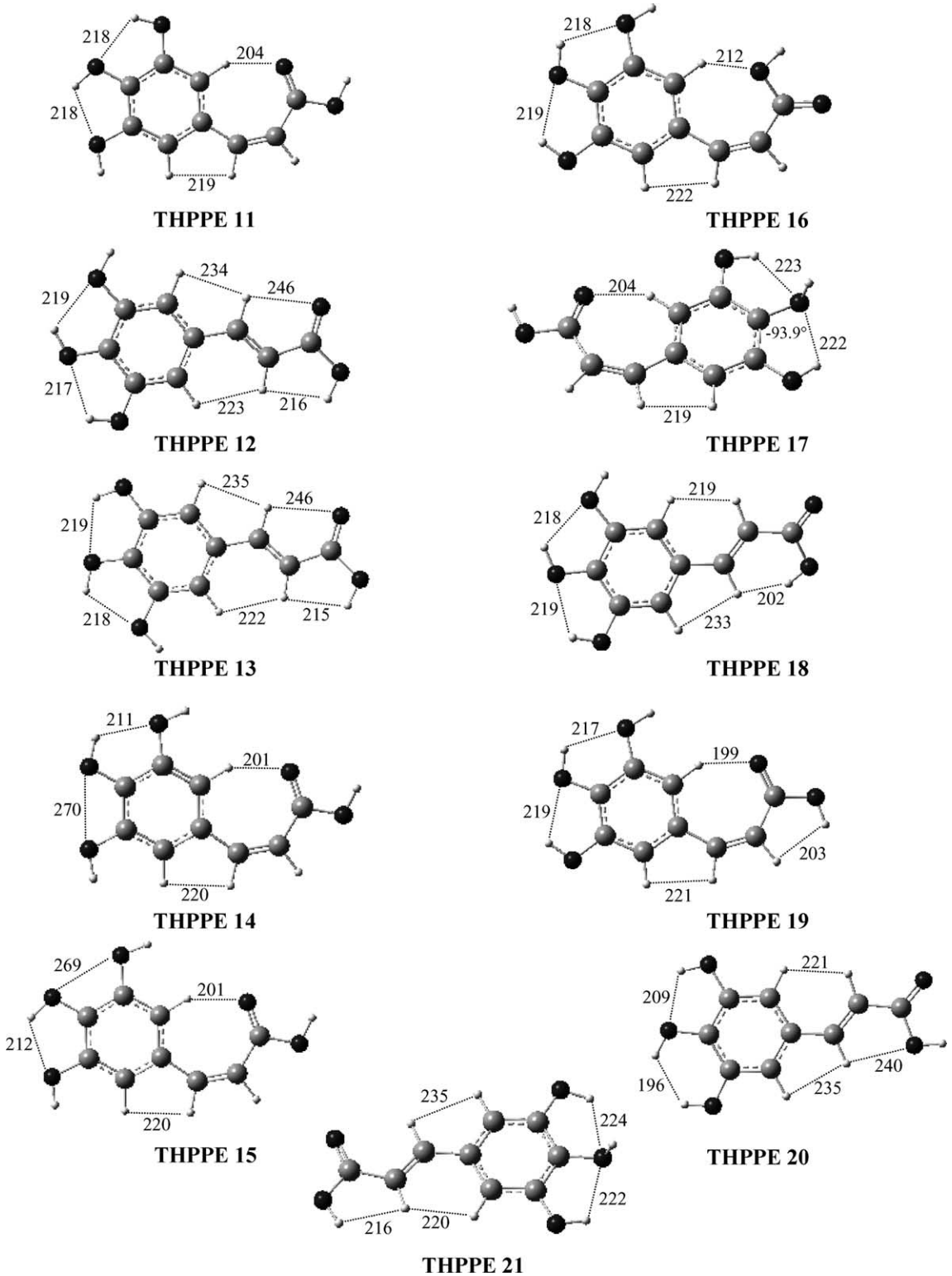

Fig. 2 (*continued*)

an S-*cis* carboxylate, and a single-directioned orientation of the ring hydroxyls. The higher energy of THPPE 19, in turn, is due to the S-*trans* orientation of its carboxylic group, which causes a serious steric hindrance between hydrogens H_{20} and H_{21} ($H_{20}\cdots H_{21}$ equal to 203 pm, Fig. 2). Moreover, H-type bonds between H_{15} and the carbonyl oxygen (O_{12}) were found to be preferred over those formed with the hydroxylate O_{21} atom-THPPE 6 ($\Delta E = 11.5$ kJ mol^{-1}, ($O_{12}\cdots H_{15}$) = 201 pm) vs THPPE 16 ($\Delta E = 29.9$ kJ mol^{-1}, ($O_{21}\cdots H_{15}$) = 212 pm) (Fig. 2).

Also, the conformers with a ($C_{10}C_9C_3C_2$) dihedral equal to 180° were found to be favoured relative to the ones with ($C_{10}C_9C_3C_2$) = 0°, possibly due to both π-delocalisation and steric repulsion effects-e.g. THPPE 1 ($H_{16}\cdots H_{20}$ = 223 pm) vs THPPE 3 ($H_{15}\cdots H_{20}$ = 219 pm) (Figs. 1 and 2). These conformational preferences are in accordance with previous results obtained for caffeic acid [25].

Table 1 comprises the calculated optimised geometries for the lowest energy conformers of THPPE (values for the other conformers are available from the authors upon request). These structural parameters do not deviate much from the X-ray values found in the literature for the analogous dihydroxylated caffeic acid [43]. Also, they are in very good agreement with the results obtained from a complete conformational analysis reported for caffeic acid [25], as well as with those calculated by Bakalbassis et al. (at the B3LYP/6-31 + G* level) for one of caffeic acid's ground-state geometries [24].

Potential-energy profiles and energy barriers for internal rotation around several bonds within the THPPE molecule—O_7–C_6, C_3–C_9, C_{10}–C_{11}, and C_{11}–O_{13}—were obtained, by scanning the corresponding torsional angles (Fig. 3).

The ($H_{18}O_7C_6C_5$) dihedral defines the orientation of the central ring hydroxyl group relative to the aromatic plane, i.e. the internal rotation around the O_7–C_6 bond. The corresponding potential-energy profile (Fig. 3A), clearly evidences the preference for a planar geometry, once the term in 180° was found to be strongly stabilising—$V_1^{180^\circ} = -45.9$ kJ mol^{-1}, as compared to the cosine terms in 90° and 60°—$V_2^{90^\circ} = -0.7$ kJ mol^{-1} and $V_3^{60^\circ} = -3.3$ kJ mol^{-1}, respectively. Also, it was verified that the most unfavoured geometries correspond to ($H_{18}O_7C_6C_5$) equal to either 0° or 360°, which is easily understandable in view of the significant steric hindrance between H_{18} and H_{17} ($H_{18}\cdots H_{17}$ equal to 149 pm, $O_7\cdots O_{14}$ being 272 pm). In fact, due to the planarity of the OH groups relative to the ring (imposed during the scanning process), the $H_{18}\cdots H_{17}$ repulsion is much more pronounced than, for instance, in conformer THPPE 20, where the $H_{18}\cdots H_{17}$ distance is equal to 196 pm and a $O_7\cdots H_{22}$ intramolecular bond can be formed (($O_7\cdots H_{22}$) = 209 pm, Fig. 2). Furthermore, values of either 180° or 0° for the three ($H_{18}O_7C_6C_1$), ($H_{17}O_8C_5C_4$) or ($H_{22}O_{14}C_1C_6$) dihedral angles, simultaneously, yield very stable conformations (e.g. THPPE 1 and THPPE 2, Fig. 2), where $H_{18}\cdots O_{14}/H_{17}\cdots O_7$, and $H_{22}\cdots O_7/H_{18}\cdots O_8$ intramolecular interactions may occur (H···O varying from 217 to 219 pm). For different values of those dihedrals, however, the strong steric hindrance between atoms H_{17} and H_{18}, and/or H_{18} and H_{22}, leads to a pronounced deviation from planarity of some of the ring hydroxyl groups (e.g. THPPE 17, ($H_{18}O_7C_6C_5$) = −93.9°, Fig. 2). The internal rotational energy barrier from ($H_{18}O_7C_6C_5$) = 180–0° (or 360°) was thus calculated to be rather high −49.1 kJ mol^{-1}. The scanning of dihedral ($H_{18}O_7C_6C_5$) was carried out for a particular conformation of the two neighbouring OH

Table 1
Relative energies and optimised geometries for the most stable conformers of 3-(3,4,5-trihydroxyphenyl)-2-propenoic acid (THPPE). (B3LYP/6-31G** level of calculation)

ΔE (kJ mol^{-1})/[a]μ (D)	THPPE 1 [b]0.00; 3.5	THPPE 2 0.45; 4.7	THPPE 3 3.47; 3.3
Bond lengths (pm)			
[c]C_1–C_6	139.6	139.8	140.1
C_2–C_1	139.0	139.4	138.7
C_3–C_2	140.9	140.5	141.0
C_3–C_9	145.9	145.9	146.1
C_4–C_3	140.7	141.0	140.5
C_5–C_4	139.0	138.7	139.4
C_6–C_5	140.2	140.1	139.8
C_9–C_{10}	134.7	134.7	134.8
C_{10}–C_{11}	147.2	147.1	146.9
C_1–O_{14}	137.5	136.1	137.5
C_5–O_8	136.1	137.5	136.1
C_6–O_7	136.8	136.8	136.8
C_{11}–O_{12}	121.8	121.7	121.8
C_{11}–O_{13}	136.1	136.2	136.2
C_2–H_{15}	108.7	108.5	108.6
C_4–H_{16}	108.3	108.6	108.5
C_9–H_{19}	108.9	108.9	108.7
C_{10}–H_{20}	108.4	108.5	108.5
O_7–H_{18}	96.9	96.9	96.9
O_8–H_{17}	96.9	96.5	96.9
O_{13}–H_{21}	97.2	97.2	97.1
O_{14}–H_{22}	96.5	96.9	96.5
Bond angles (°)			
C_2–C_3–C_4	119.2	119.2	119.2
C_9–C_3–C_2	118.0	118.2	122.7
C_{10}–C_9–C_3	128.0	128.0	127.5
C_{11}–C_{10}–C_9	119.8	120.0	124.0
O_8–C_5–C_6	119.9	114.3	120.3
O_{13}–C_{11}–C_{10}	111.5	111.5	114.0
O_{13}–C_{11}–O_{12}	122.0	122.0	121.8
H_{17}–O_8–C_5	107.9	109.9	107.8
H_{19}–C_9–C_{10}	115.9	116.1	117.3
H_{20}–C_{10}–C_9	123.3	123.3	122.8
H_{21}–O_{13}–C_{11}	105.6	105.6	105.3
H_{22}–O_{14}–C_1	109.9	107.9	109.9
Dihedral angles (°)			
C_3–C_4–C_5–C_6	0.0	0.0	0.0
C_9–C_3–C_4–C_5	−180.0	180.0	180.0
C_{10}–C_9–C_3–C_2	−180.0	−180.0	0.0
C_{11}–C_{10}–C_9–C_3	180.0	180.0	180.0
O_{12}–C_{11}–C_{10}–C_9	0.0	0.0	180.0
O_{13}–C_{11}–C_{10}–C_9	−180.0	180.0	0.0
H_{15}–C_2–C_3–C_9	0.0	0.0	0.0
H_{16}–C_4–C_3–C_2	180.0	180.0	180.0
H_{17}–O_8–C_5–C_6	0.0	−180.0	0.0
H_{18}–O_7–C_6–C_1	0.0	−180.0	0.0
H_{20}–C_{10}–C_9–C_3	0.0	0.0	0.0
H_{21}–O_{13}–C_{11}–C_{10}	180.0	−180.0	180.0
H_{22}–O_{14}–C_1–C_2	0.0	180.0	0.0

[a] Total dipolar moment 1D = 1/3 × 10^{-2} Cm.
[b] Total value of energy for the most stable conformer of THPPE is −723.904147480 (in Hartree, 1 Hartree = 2625.5001 kJ mol^{-1}).
[c] Atoms are numbered according to Fig. 1.

groups—($H_{17}O_8C_5C_4$) and ($H_{22}O_{14}C_1C_6$) equal to 180°—once, as expected, variation of the orientation of one of them affects the position of the others. This conformational behaviour of the ring hydroxyls in THPPE differs from the one encountered for caffeic acid [25], on account of the presence of three OH ring substituents in the latter, in a symmetric position relative to the pendant carbon chain. This explains the ocurrence of a maximum energy geometry for ($H_{18}O_7C_6C_5$) = 0/360°, as opposed to caffeic acid, for which the absence of the third hydroxyl allows a certain stabilisation in these conditions, the most unfavourable conformation corresponding to ($H_{18}O_7C_6C_5$) = 90° ($V_1^{180°} = -45.9$ vs -15.1 kJ mol^{-1}, and $V_2^{90°} = -0.7$ vs 22.3 kJ mol^{-1}, respectively, for THPPE and CA). Actually, the presence of three OH ring substituents is prone to affect the electronic delocalisation process within the THPPE molecule, as compared to the dihydroxylated analogue.

The orientation of the pendant carbon chain relative to the aromatic ring is defined by dihedral ($C_{10}C_9C_3C_2$)—e.g. THPPE 1 (($C_{10}C_9C_3C_2$) = 0°) and THPPE 7

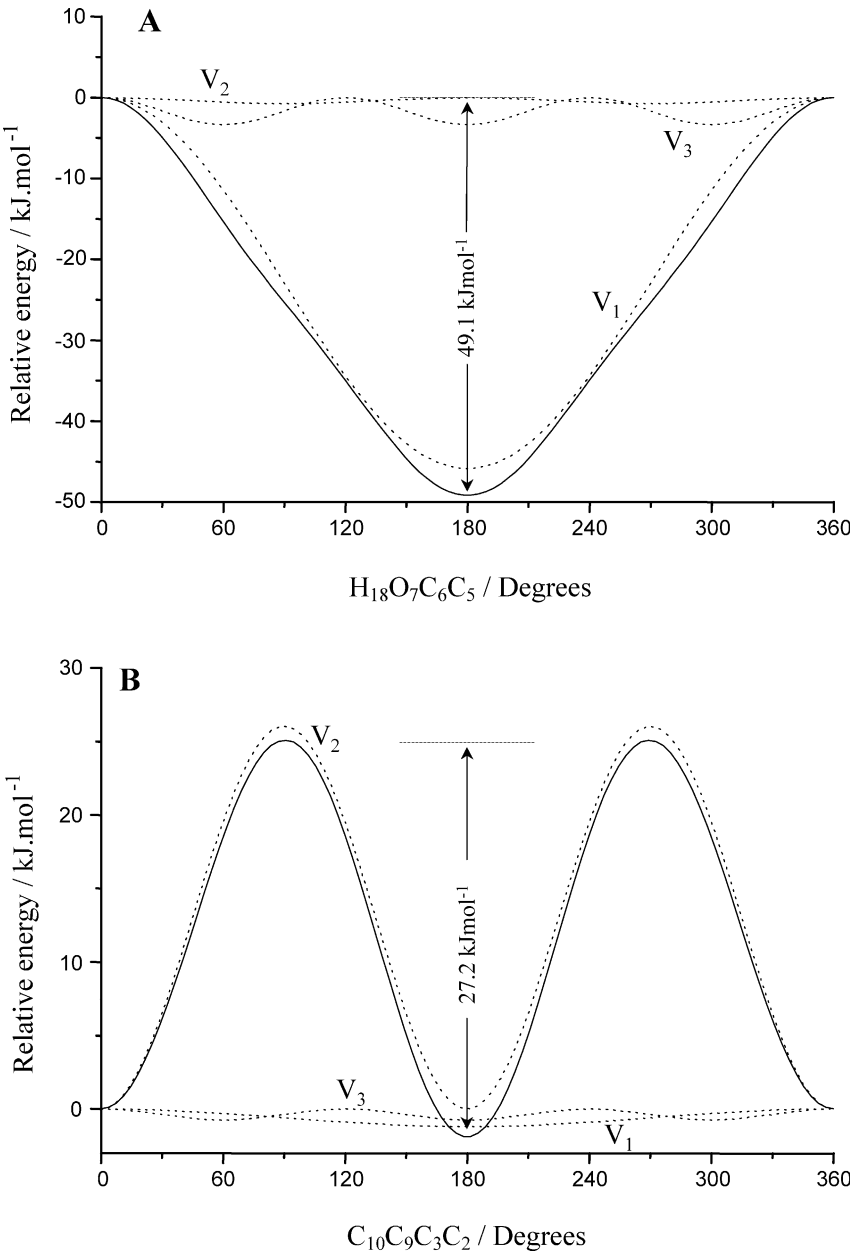

Fig. 3. Optimised conformational energy profiles, and their Fourier deconvolutions, for several internal rotations within the 3-(3,4,5-trihydroxyphenyl)-2-propenoic acid (THPPE) molecule. A − around the O_7-C_6 bond: $V_1 = -45.9$ kJ mol^{-1}, $V_2 = -0.7$ kJ mol^{-1}, $V_3 = -3.3$ kJ mol^{-1}. B—around the C_9-C_3 bond: $V_1 = -1.2$ kJ mol^{-1}, V_2 =26.0 kJ mol^{-1} and $V_3 = -0.7$ kJ mol^{-1}. C—around the $C_{11}-C_{10}$ bond: V_1 =1.9 kJ mol^{-1}, $V_2 = 35.6$ kJ mol^{-1}. D—around the $O_{13}-C_{11}$ bond: $V_1 = 22.8$ kJ mol^{-1}, $V_2 = 43.2$ kJ mol^{-1}. (When varying ($H_{18}O_7C_6C_5$), both ($H_{22}O_{14}C_1C_6$) and ($H_{17}O_8C_5C_4$) were frozen at 180°. B3LYP/6-31G* level of calculation).

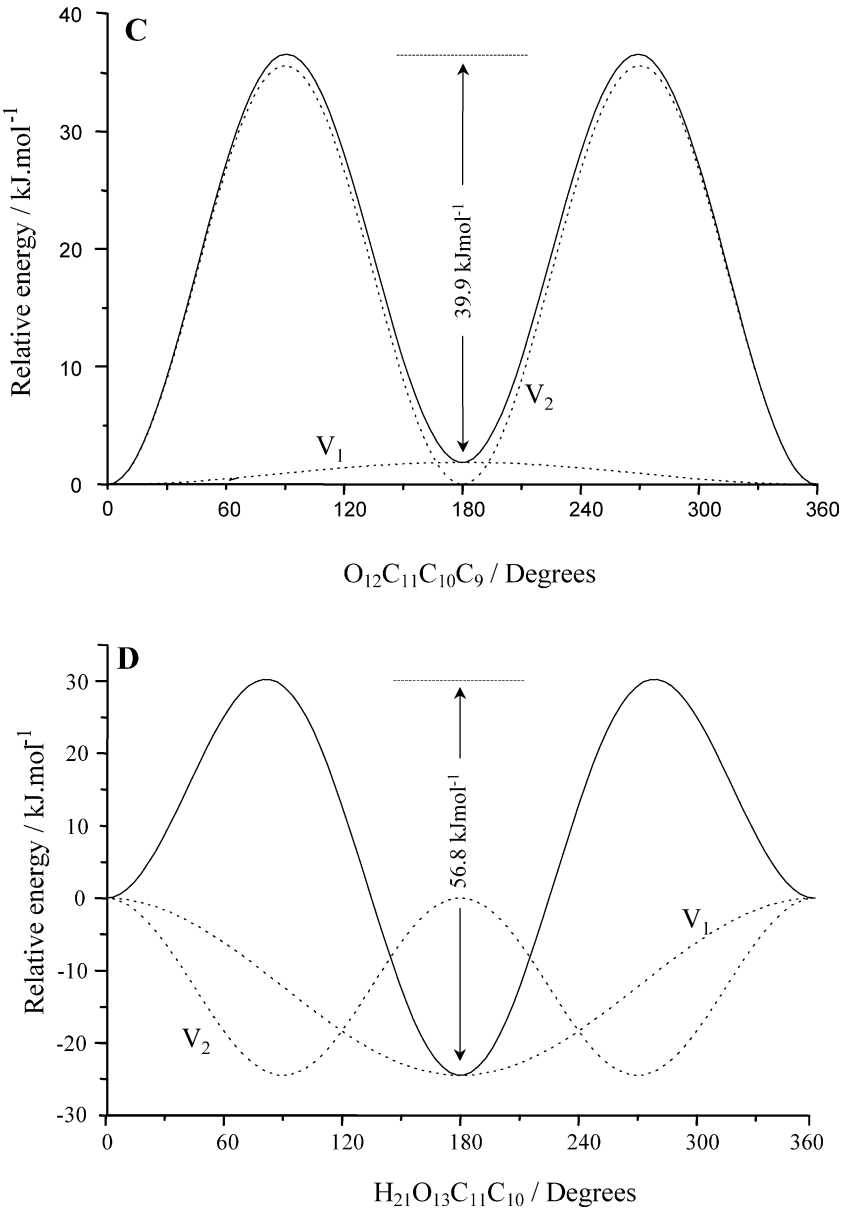

Fig. 3 (*continued*)

($(C_{10}C_9C_3C_2) = 180°$). The analysis of the Fourier components of the corresponding potential-energy variation (Fig. 3B) evidences the preference for a planar geometry, i.e. for a completely conjugated system—in fact, the cosine term in 90° (V_2) is by far the primary positive contribution to that profile ($V_2^{90°} = 26.0$ kJ mol^{-1} vs $V_1^{180°} = -1.2$ kJ mol^{-1} and $V_3^{60°} = -0.7$ kJ mol^{-1}). This may be explained by the strong stabilisation due to π-electron delocalisation, which is considerably more effective for a linear zig–zag like unsaturated pendant chain, coplanar with the aromatic ring. A value of 27.2 kJ mol^{-1} for the internal rotational energy barrier—from ($C_{10}C_9C_3C_2$) equal to 180–90° was obtained.

The variation of the ($O_{12}C_{11}C_{10}C_9$) dihedral (Fig. 3C) represents the internal rotation of the carboxylate group, around the C_{10}–C_{11} bond—e.g. geometries THPPE 1 ($(O_{12}C_{11}C_{10}C_9) = 0°$) and THPPE 4 ($(O_{12}C_{11}C_{10}C_9) = 180°$). The term in 90° was found to be the ruling unstabilising contribution ($V_2^{90°} = 35.6$ kJ mol^{-1} vs $V_1^{180°} = 1.9$ kJ mol^{-1}), the planar arrangement of the carboxylate group relative to the aromatic ring and the carbon chain double bond being once more highly favoured ($\Delta E = 39.9$ kJ mol^{-1}).

Rotation around the C_{11}–O_{13} bond, defining either an S-*cis* or S-*trans* conformation within the carboxylic group, is represented in Fig. 3D, and corresponds to the highest energy barrier calculated for this molecule ($\Delta E = 56.8$ kJ mol^{-1}). A clear preference for an S-*cis* orientation is obtained, the less favoured conformation being the one with ($H_{21}O_{13}C_{11}C_{10}$) = 90°, due to the loss of

planarity of the system—$V_2^{90°} = 43.2$ kJ mol^{-1} vs $V_1^{180°} = -22.8$ kJ mol^{-1}. In fact, the geometry displaying a 90° orientation of the carboxylic OH goup relative to the plane containing both the carbon chain and the ring corresponds to a maximum in the potential-energy profile, and not the S-*trans* geometry. Actually, the latter corresponds to a planar arrangement of the molecule, despite some steric hindrance which may occur between atoms H_{20} and H_{21} (e.g. $H_{20}\cdots H_{21}$ ca. 215 pm in THPPE 12 and 13, Fig. 2). It is thus concluded that the most stable conformations of the carboxylate moiety are the ones corresponding to $(O_{12}C_{11}C_{10}C_9) = 0°$ and $(H_{21}O_{13}C_{11}C_{10}) = 180°$—THPPE 1, THPPE 2 and THPPE 3.

The harmonic vibrational frequencies were calculated for all conformers of THPPE (data available from the authors upon request). The ones for the most stable geometries are comprised in Table 2 and show a good overall agreement with both the experimental data (after scaling according to Scott and Radom for the particular basis set used [40]), and the theoretical values previously obtained by the authors for caffeic acid [25].

In order to better mimetise THPPE in the solid state, and once this kind of phenolic carboxylic acids predominantly occur (in the condensed phase) as hydrogen-bonded dimers, calculations were also carried out for a dimeric species, formed through intermolecular top-to-top (O)H$\cdots$O(=C) interactions between the carboxylate groups of each molecule (Fig. 4, Table 2). This dimeric structure was found to be energetically favoured, displaying quite strong hydrogen close contacts-(O)H$\cdots$O(=C) distances of 162 and 163 pm.

3.2. Raman spectroscopy

Fig. 5 represents the solid state Raman spectra (at room temperature) of 3-(3,4,5-trihydroxyphenyl)-2-propenoic acid and its ethyl ester (ETHPPE), in the 150 to 1750 cm^{-1} region. The corresponding experimental Raman wavenumbers are gathered in Table 2, along with the values calculated (at the B3LYP/6-31G** level) for the two most stable conformers of THPPE and for a dimeric form of this molecule (represented in Fig. 4). Although the calculated spectrum of the dimer contains twice the number of frequencies compared to the monomer, only those presenting a better agreement with the experimental values are comprised in Table 2.

A complete assignment of the Raman bands of THPPE was performed, based on the theoretical results presently obtained for this molecule, as well as on previous studies on similar phenolic compounds [25,44] (Table 2). The main observed features were (Fig. 5): (i) C=C double bond stretching vibrations—at ca. 1640 and 1612 cm^{-1} (1661 and 1601 cm^{-1}, respectively, in the ester); (ii) aromatic ring ν_{CC} mode-at 1583 and 1612 cm^{-1} (1601 cm^{-1} in the ester); (iii) out-of-plane ring wagging vibrations—at wavenumbers from ca. 800 and 1000 cm^{-1}, typical of tri-substituted benzenes; (iv) CH deformations—both wagging, at ca. 1370 cm^{-1}, and rocking modes, at 700–870 cm^{-1}; (v) CH characteristic stretching vibrations, both symmetric and assymmetric, respectively, around 3050–3125 cm^{-1}; (vi) bands around 1290 and 1150–60 cm^{-1}, which are assigned, in THPPE, to both ν_{CO} and δ_{OH} vibrations: while in the acid species these are broad features, clearly comprising more than one mode, in the ester they are narrower, probably corresponding solely to the OH deformations.

The ν_{OH} modes—either from the carboxylic group or the hydroxyl ring substituents—were not detected experimentally for THPPE, while the ones observed for both CA and ETHPPE displayed a significant shift relative to the predicted values (Table 2). In fact, formation of stabilising (O)H$\cdots$O(=C) intermolecular close contacts in this kind of phenolic compounds is known to occur, yielding rather stable dimeric species, and giving rise to downward frequency shifts of both the $\nu_{C=O}$ and ν_{OH} modes (as previously observed for substituted benzaldehydes [45,46]). Raman spectra of THPPE in solution was thus obtained, in view of better understanding the behaviour of the carboxylic $\nu_{C=O}$ oscillator upon dilution (e.g. decrease of the dimer:monomer ratio). DMSO-d_6 was chosen as a suitable solvent for this purpose, as it does not display any bands in the spectral region of interest. Moreover, any interaction that might occur between the THPPE molecule and DMSO—via (O)H$\cdots$O(=S) close contacts—was detected only for very high dilutions, through a band appearing at ca. 1750 cm^{-1} [47], which did not interfere with the features under study. Two bands ascribed to the C=O stretching mode—at both 1692 and 1636 cm^{-1}—were detected for the THPPE-DMSO-d_6 solution (40 mM), as opposed to the solid, for which only the feature at lower wavenumber (1640 cm^{-1}) was to be seen with significant intensity (Table 2, Fig. 6). These two bands are suggested to be due to the free and hydrogen-bonded forms of the C=O group, respectively. Actually, while the dimeric species is expected to be predominant in the solid ($\nu_{C=O} = 1640$ cm^{-1}), dilution may be responsible for the presence of the monomeric form, which is reflected by the observation of free carboxylate groups (not involved in intermolecular H-bonds)—$\nu_{C=O}$ vibration (1692 cm^{-1}). The higher electronic delocalisation occuring in THPPE (due to the presence of the linear chain double bond) relative to the aromatic aldehydes previously reported [45,46] leads to a larger shift (ca. 50 cm^{-1}) then the one measured for benzaldehyde dimers (ca. 10 cm^{-1}). Also, as expected for this kind of dimeric–monomeric carboxyl modes, the C–O stretching vibration was found to be shifted from 1289 to 1267 cm^{-1}, when going from the solid state to the solution (Fig. 6). The OH bending vibration, detected at about 1355 cm^{-1} in the solution, is also typical of monomeric forms, while the corresponding mode for dimers appears at slightly higher values (at 1374 cm^{-1}). The band appearing at 1462 cm^{-1} in the spectrum of the solution, which is assigned to both C–O

Table 2
Experimental (solid state) and calculated (B3LYP/6-31G**) Raman wavenumbers (cm^{-1}) for the most stable conformers of 3-(3,4,5-trihydroxyphenyl)-2-propenoic acid (THPPE), as well as for a THPPE 1 dimeric structure. (Values for CA and ETHPPE are included for comparison)

Experimental			Calculated[a]				Approximate description[b]
THPPE	CA	ETHPPE	THPPE 1[c](44%)	THPPE 2 (37%)	THPPE 1-Dimer	CA[d]	
			3696 (72;117)	3695 (64;98)	3696 (71;117)	3693 (61; 98)	$\nu\,(O_{14}H_{22})$
	3368	3370	3648 (140;180)	3646 (126;159)	3648 (110;280)	3627 (123;177)	$\nu\,(O_7H_{18})$
	3341	3341	3637 (99;100)	3640 (101;108)	3637 (76;146)		$\nu\,(O_8H_{17})$
	3321	3321	3619 (87;198)	3619 (88;196)		3619 (89;193)	$\nu\,(O_{13}H_{21})$
3124			3101 (3;55)	3091 (2;65)	3102 (2;52)	3095 (6;169)	$\nu\,(CH)_{ring\ +}\ +\ \nu\,(CH)_{chain}$
3080	3084		3089 (4;14)	3084 (10;48)	3091 (0;24)	3084 (11;36)	$\nu\,(CH)_{chain}$
3067	3079	3064	3059 (8;71)	3068 (4;22)	3058 (6;88)	3073 (5;62)	$\nu\,(CH)_{ring}$
3053	3040		3045 (1;27)	3051 (1;34)	3048 (2;22)	3058 (8;25)	$\nu\,(CH)_{chain}$
	3033	3035				3049 (1;31)	$\nu\,(CH)$
					2879 (2;2879)		$\nu\,(O_{13}H_{21})$
	3026						$\nu\,(CH)$
3020							$(1289 + 1612/1640)\ cm^{-1}$
	2992	3009					$\nu\,(CH)$
		2988					
		2966					
		2942					
		2899					
1697			1739 (258;85)	1742 (266;92)	1690 (481;0)	1741 (270;87)	$\nu\,(C{=}O)$
1640	1640	1660	1634 (218;659)	1631 (239;704)	1646 (0;664)	1630 (208;699)	$\nu\,(C{=}C)$
1612	1613				1629 (1;1482)		$\nu\,(C{=}C) + \nu\,(C{=}O) + \nu\,(CC)_{ring}$
		1602	1601 (157;1606)	1605 (75;509)	1601 (0;4433)	1599 (271;1481)	$\nu\,(CC)_{ring+}\nu\,(C{=}C)_{chain}$
1583	1595		1599 (157; 1606)	1597 (194;1052)	1599 (1;1121)	1584 (29;22)	$\nu\,(CC)_{ring}$
	1532						
	1525	1512	1517 (133;18)	1518 (209;1)	1517 (0;1)	1512 (178;2)	$\nu\,(CC)_{ring}$
		1476	1459 (232;3)	1455 (81;14)		1436 (177;144)	$\nu\,(CC)_{ring} + \delta\,(O_8H_{17})$
					1464 (0;164)		$\delta\,(O_8H_{17}) + \delta\,(O_{13}H_{21}) + \delta\,(CH)_{chain}$
					1457 (0;710)		$\delta\,(OH)$
1374		1386	1375 (22;96)	1378 (50;125)		1379 (128;35)	$\nu\,(CC)_{ring} + \delta\,(OH)_{ring} + \delta\,(CH)_{chain}$
					1365		$\nu\,(CC)_{ring} + \delta\,(O_8H_{17}) + \delta\,(O_{13}H_{21}) + \delta\,(CH)_{chain}$
					1358		$\nu\,(CC)_{ring} + \delta\,(O_8H_{17}) + \delta\,(O_{13}H_{21}) + \delta\,(CH)_{chain}$
1355	1354		1362 (1;99)	1354 (174;146)		1344 (31;2)	$\nu\,(CC)_{ring} + \delta\,(O_7H_{18}) + \delta\,(CH)$
	1316	1316	1329 (33;39)	1339 (24;2)		1314 (0;43)	$\delta\,(O_8H_{17}) + \delta\,(O_{13}H_{21}) + \delta\,(CH)_{chain}$
1307	1299		1306 (157;2)	1308 (167;11)		1295 (18;6)	$\nu\,(CC)_{ring} + \nu\,(CO) + \delta\,(CH) + \delta\,(OH)_{ring} + \delta\,(OH)_{carbox}$
1289	1286	1282	1292 (428;140)	1275 (280;80)	1311 (0,82)	1277 (379;32)	$\delta\,(OH)_{ring} + \delta\,(OH)_{carbox} + \delta\,(CH)$
1245			1261 (178;46)	1270 (128;28)	1296 (961;9)	1250 (10;94)	$\nu\,(CC)_{ring} + \nu\,(CO) + \delta\,(CH) + \delta\,(OH)_{ring} + \delta\,(OH)_{carbox}$
1236			1221 (118;18)	1221 (74;11)		1223 (4;7)	$\nu\,(CC)_{ring} + \nu\,(CO) + \delta\,(CH) + \delta\,(CH) + \delta\,(OH)_{ring} + \delta\,(OH)_{carbox}$
1204	1186	1204	1212 (17;20)	1214 (85;11)		1173 (145;118)	$\delta\,(CH) + \nu\,(C_5O_8) + \delta\,(O_7H_{18}) + \delta\,(O_8H_{17}) + \delta\,(O_{13}H_{21})$
1151	1177	1151	1177 (84;2)	1170 (95;4)		1147 (5;47)	$\delta\,(O_7H_{18}) + \nu\,(CH) + \nu\,(CO)$
1141			1138 (120;5)	1135 (36;51)		1129 (129;7)	$\delta\,(O_{13}H_{21}) + \delta\,(O_{14}H_{22}) + \delta\,(CH)$
					1136 (0;541)		$\delta\,(OH)_{ring} + \delta\,(CH)$
					1131 (24;97)		$\delta\,(OH)_{ring} + \delta\,(CH)$

(*continued on next page*)

Table 2 (*continued*)

Experimental			Calculated[a]				Approximate description[b]
THPPE	CA	ETHPPE	THPPE 1[c](44%)	THPPE 2 (37%)	THPPE 1-Dimer	CA[d]	
	1122	1122	1132 (3;60)	1130 (39;1)		1108 (625;201)	$\delta\,(O_7H_{18}) + \delta\,(O_{14}H_{22}) + \delta\,(CH)_{ring}$
			1105 (103;3)	1103 (665; 280)		1091 (128;30)	$\delta\,(O_{13}H_{21}) + \delta\,(O_{14}H_{22}) + \delta\,(CH)$
1005	1006	1006	1015 (573;284)	1014 (149;3)	1015 (46;18)	992 (21;3)	$\nu\,(CC)_{ring} + \nu\,(CO)_{ring}\,\delta\,(CH) + \delta\,(OH)_{ring}$
992			991 (198;9)	991 (22;2)	990 (14;3)	957 (15;8)	$\gamma\,(CH)_{chain}$
972			974 (6;6)	976 (5;8)	976 (0;10)	930 (15;6)	$\nu\,(CC)_{ring} + \delta\,(CCC)_{chain}$
			935 (16;9)	935 (32;11)		907 (1;3)	$\nu\,(CC)_{ring} + \nu\,(CC)_{ring} + \delta\,(OH)$
					925 (0;2)		$\gamma\,(O_{13}H_{21})$
					850 (0;36)		$\delta\,(CCC)_{chain}$
868	874	872	847 (12;13)	847 (4;12)		843 (5;10)	$\gamma\,(C_{10}H_{20})$
	854	854					
810	812	811	819 (12;2)	822 (30;2)		811 (48;1)	$\gamma\,(C_4H_{16})$
					820 (5;3)		$\gamma\,(CH)_{ring}$
					784 (0;52)		$\delta\,(CCC)$
			782 (20;19)	782 (11;21)		796 (14;6)	$\nu\,(CC)_{ring} + \nu\,(CO)_{ring}$
		761	775 (41;1)	765 (29;2)		785 (5;29)	$\gamma\,(C_2H_{15})$
739	740	741	721 (24;2)	721 (27;2)		747 (9;8)	$\gamma\,(C_2H_{16}) + \gamma\,(CCC)_{chain}$
671			678 (2;3)	679 (4;3)	696 (0;4)	721 (24;3)	$\nu\,(CC)_{ring} + \delta\,(CCC)_{chain}$
665	647	647					
624	622	623	616 (11;3)	614 (39;2)	619 (0;17)	625 (22;13)	$\delta\,(CCC)_{chain}$
605			608 (61;6)	608 (65;6)		603 (69;4)	$\gamma\,(O_{13}H_{21}) + \Gamma\,(CCC)$
589			581 (82;12)	581 (56;14)		579 (28;5)	$\Delta\,(CCC)_{ring} + \Delta\,(CCC)_{chain}$
			558 (26;2)	559 (26;2)		560 (26;4)	$\Delta\,(CCC)_{ring} + \Delta\,(CCC)_{chain} + \gamma\,(O_{13}H_{21})$
541	541	541				528 (46;1)	$\Delta\,(CCC)_{ring} + \gamma\,(O_{13}H_{21})$
521		502	522 (0;4)	521 (1;4)	524 (0;9)	498 (12;1)	$\Delta\,(CCC)_{ring} + \delta\,(CCC)_{chain}$
484		481	489 (25;6)	489 (32;6)	499 (0;26)	454 (76;3)	$\Delta\,(CCC)$
452			454 (11;3)	454 (4;2)	462 (0;6)	439 (13;3)	$\Delta\,(CCC)$
434			426 (51;1)	415 (39;2)	423 (42;2)		$\gamma\,(O_8H_{17}) + \gamma\,(O_7H_{18})$
380		395	387 (20;5)	386 (16;4)	388 (0;8)	381 (1;2)	$\Gamma\,(CCC)$
352		352	357 (104;2)	360 (123;3)	357 (117;2)		$\gamma\,(O_{14}H_{22}) + \gamma\,(O_8H_{17}) + \gamma\,(O_7H_{18})$
323			316 (10;1)	316 (12;1)	301 (0;5)		$\Delta\,(COH)_{ring}$
290				296 (1;1)	292 (0;17)	290 (4;2)	$\Delta\,(COH)_{ring}$
		274	276 (2;4)	277 (1;2)	274 (0;3)	247 (10;4)	$\Delta\,(CCC)$
264		262	251 (7;1)	250 (5;4)	252 (0;2)	205 (2;5)	$\Gamma\,(CCC)$
241		229	213 (0;3)	214 (174;2)		–	$\Delta\,(CCC)_{chain}$
			209 (179;5)	213 (2;4)	207 (49;8)	216 (139;1)	$\gamma\,(O_7H_{18}) + \gamma\,(O_{14}H_{22})$
179		177	162 (0;1)	161 (0;1)	176 (0;7)	187 (15;0)	$\Gamma\,(CCC)$
					163 (0;8)		$\Delta\,(CCC)$
		141	137 (1;1)	135 (1;1)		134 (0;2)	skeletal modes
						37 (0;10)	skeletal modes
						33 (0;1)	skeletal modes

[a] Wavenumbers above 400 cm^{-1} are scaled by a factor of 0.9614 [40]. (IR intensities in km mol^{-1}; Raman scattering activities in Å.amu).

[b] Atoms are numbered according to Fig. 1.

[c] Relative population (at 25 °C).

[d] [25].

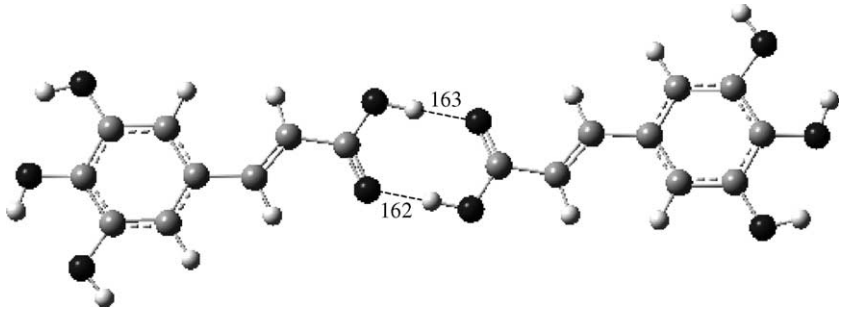

Fig. 4. Representation of a calculated dimeric structure for 3-(3,4,5-trihydroxy-phenyl)-2-propenoic acid (THPPE). (B3LYP/6-31G** level of calculation. Distances are represented in pm).

stretching and in-plane C–O–H deformation – thus being directly affected by the occurrence of dimeric structures (Fig. 4)-is not observed in the condensed phase. As to the aromatic ring $\nu_{C=C}$ mode, it suffers a slight downward shift when going from the dimer (1612 cm^{-1}) to the monomer (1605 cm^{-1}). An identical behaviour was observed for caffeic acid (CA), the dihydroxylated analogue of THPPE, which is well known for forming dimeric structures in the solid phase [48,49].

Furthermore, the fact that no experimental ν_{OH} Raman bands were seen in the spectrum of solid THPPE is characteristic of the presence of dimeric species, for which these vibrations yield extremely broad features at around 3300 cm^{-1}, often not detected, as a consequence of the formation of intermolecular H-bonds involving those hydroxyl groups. These findings are corroborated by the Ab initio results obtained for a THPPE dimeric structure. As expected, the calculated wavenumbers associated to the groups involved in intermolecular hydrogen close-contacts within the dimer (e.g. carboxylic C=O) presented a better accordance with the experimental values obtained for the solid than the ones calculated for the isolated molecule. In fact, both $\nu_{C=O}$ experimental bands—at 1697 and 1640 cm^{-1}-were predicted by the calculations when considering the dimer—at 1690 cm^{-1} and 1646 cm^{-1}, respectively—but not when considering the monomer (Table 2). Moreover, characteristic bands of the dimeric species were obtained by the calculations, namely at

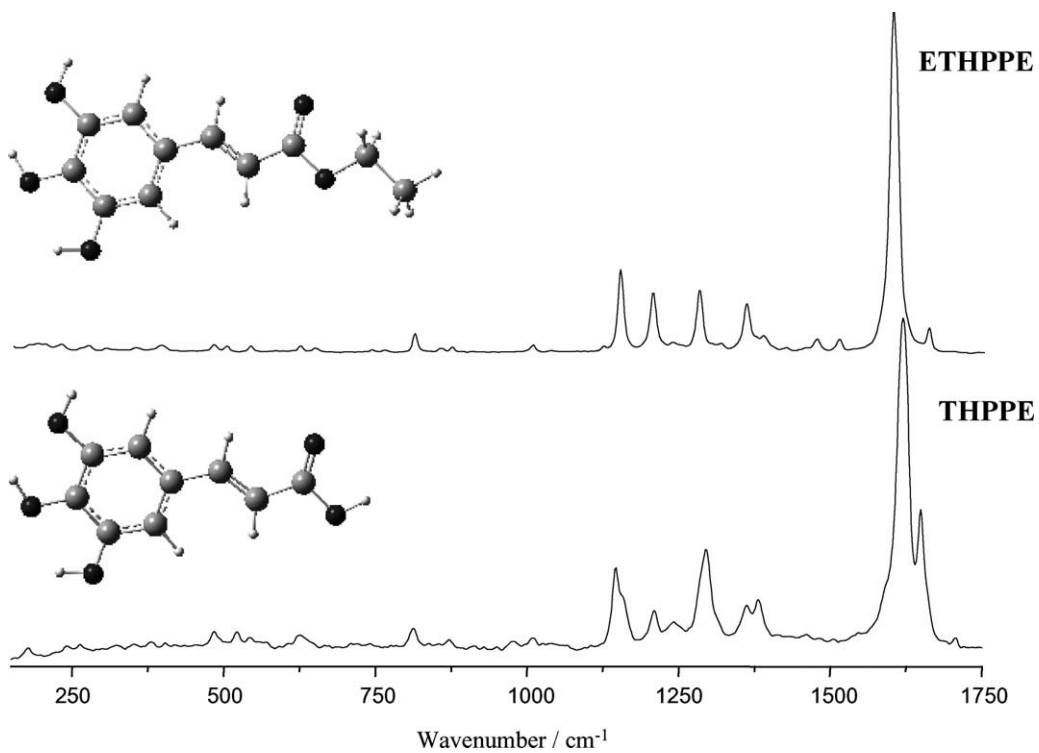

Fig. 5. Experimental Raman spectra (150-1750 cm^{-1}) of 3-(3,4,5-trihydroxyphenyl)-2-propenoic acid (THPPE) and the corresponding ethyl ester (ETHPPE). (Solid state, at 25 °C).

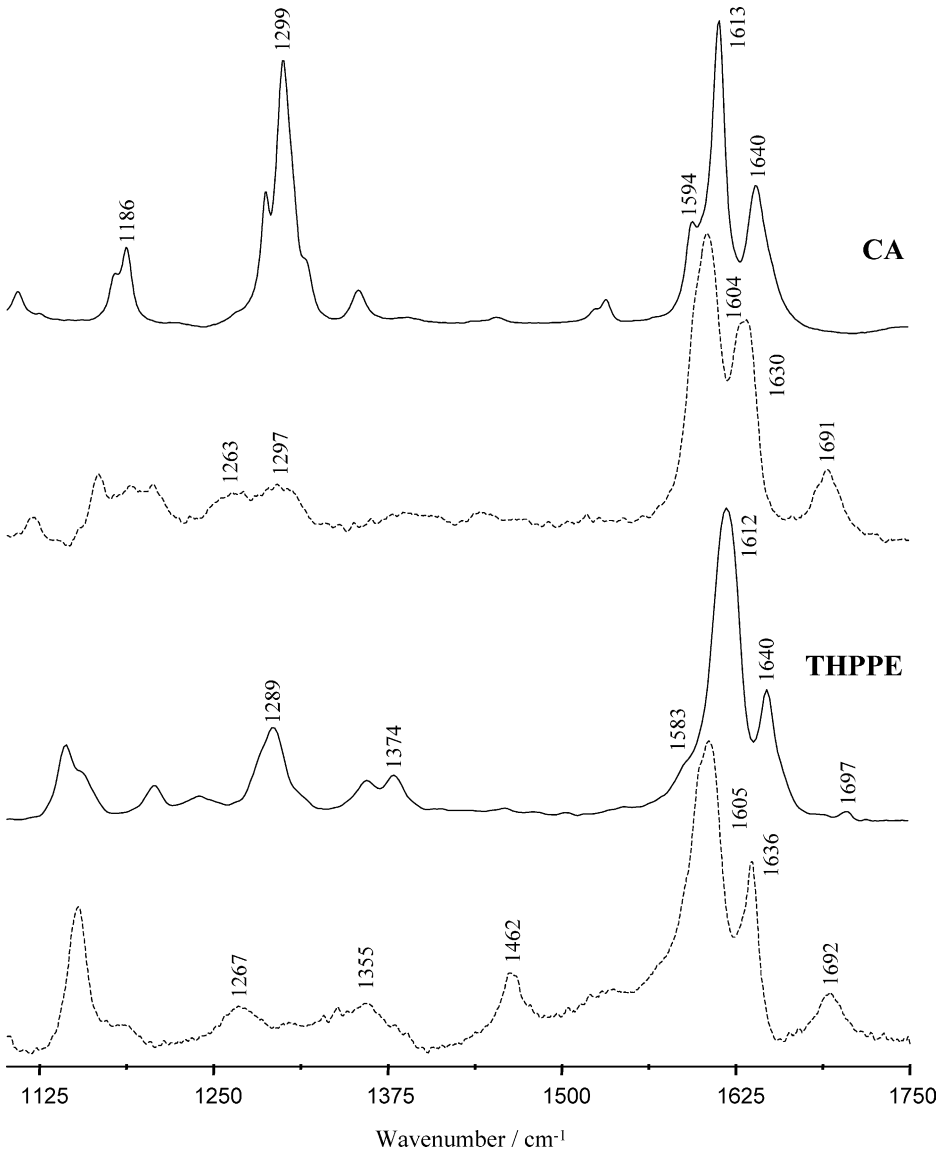

Fig. 6. Experimental Raman spectra (1100–1750 cm^{-1}, at 25 °C) of 3-(3,4,5-trihydroxyphenyl)-2-propenoic acid (THPPE) and the analogous dihydroxylated caffeic acid (CA), both in the solid state and in DMSO-d_6 solution (40 mM). (Solid line-solid state; dotted line-solution).

2879 cm^{-1}—assigned to ν_{OH} involved in (O)H···O(=C) and/or (O)H···O(H) intermolecular bonds—and at 1464, 1457 and 925 cm^{-1}—ascribed to in-plane and out-of-plane OH bending modes (Table 2). The similarity between the Raman pattern obtained for the ETHPPE ester and the THPPE solution (except for the C=O stretching mode, Fig. 5), is good evidence of the validity of the previously discussed assignment for the phenolic acid—two distinct signals for $\nu_{C=O}$ in the solid, due to the monomer and dimer species.

The agreement between the results now obtained for THPPE—both calculated and experimental vibrational wavenumbers—and the data found in the literature for similar molecules, both from theoretical and spectroscopic studies [25,44,48–50], was found to be quite good.

4. Conclusions

The conformational analysis performed for THPPE rendered twenty one distinct conformers, with structural differences concerning the conformation of the terminal carboxylate group and the pendant carbon chain, as well as the orientation of the three ring hydroxyl substituents. Two of these conformers—THPPE1 ($\Delta E = 0.0$ kJ mol^{-1}) and THPPE2 ($\Delta E = 0.5$ kJ mol^{-1})—were found to be significantly more stable, with populations at room temperature of 44 and 37%, respectively. It was verified that the lowest energy species displayed a planar geometry (C_S symmetry), as well as a carboxylate S-*cis* conformation. In fact, these two factors—carboxylate terminal group orientation and coplanarity of the molecule—appear to be the most

significant stabilising factors in this kind of systems: The preference for planarity is predictable, once it favours electron delocalisation through the expanded π system of the hyperconjugated molecule of THPPE. Thus, non-planar geometries arose only in order to overcome steric hindrance destabilising factors, whose minimisation resulted to be more favorable then the maintenance of planarity. Potential-energy profiles for internal rotation around different bonds within the molecule also supported the energetically favoured planar arrangement.

The Raman data presently obtained for THPPE is in total agreement with previous studies on similar phenolic compounds [25,44]. The presence of dimeric species in the solid state (predicted by the calculations) was clearly evidenced in the Raman pattern obtained for both the condensed phase and the solution, mainly through the characteristic low frequency shifts detected for both the $\nu_{C=O}$ and ν_{C-O} vibrational modes.

In conclusion, this kind of vibrational spectroscopic studies carried out for phenolic acids, coupled to Ab initio theoretical calculations, are of the utmost importance for understanding the structure-activity relationships ruling the biological activity of such compounds, which, apart from being recognised antioxidants, often reveal cytotoxic properties against human cancer cell lines. Actually, cytotoxic and growth-inhibition assays with both THPPE and analogous compounds displaying potential anti-cancer activity (e.g. caffeic and gallic acids, as well as some of their esters) are presently being performed in our laboratory [17], and can only be accurately interpreted in the light of the corresponding conformational analysis.

Acknowledgements

SF and MPM thank the Chemistry Department of the University of Aveiro (in the person of Dr Helena Nogueira), where the FT-Raman experiments were carried out. NM is grateful to FCT for a fellowship (PRAXIS XXI/BD/18520/98).

References

[1] O.I. Aruoma, A. Murcia, J. Butler, B. Halliwell, J. Agric. Food Chem. 41 (1993) 1880.
[2] C.A. Rice-Evans, N.J. Miller, G. Paganga, Free Rad. Biol. Med. 20 (1996) 933.
[3] G. Cao, E. Sofic, R.L. Prior, Free Rad. Biol. Med. 22 (1997) 749.
[4] V.L. Singleton, Am. J. Enol. 38 (1987) 69.
[5] P. Groupy, A. Fleuriet, M.J. Amiot, J.J. Macheix, J. Agric. Food Chem. 39 (1991) 92.
[6] M. Brenes-Balbuena, P. García-García, A. Garrido-Fernandez, J. Agric. Food. Chem. 40 (1992) 1192.
[7] A. Serrano, C. Palacios, G. Roy, C. Cespón, M.L. Villar, M. Nocito, P. González-Porqué, Arch. Biochem. Biophys. 350 (1) (1998) 49.
[8] F.A.M. Silva, F. Borges, M.A. Ferreira, J. Agric. Food Chem. 49 (2001) 3936.
[9] H. Esterbauer, J. Gebicki, H. Puhl, G. Jurgens, Free Rad. Biol. Med. 13 (1992) 341.
[10] B. Halliwell, J.C. Gutteridge, Free Radicals in Biology and Medicine, Oxford Science Publications, 1999.
[11] S. Passi, M. Picardo, M. Nazzaro-Porro, Biochem. J. 245 (1987) 537.
[12] T. Nakayama, Cancer Res. 54 (Suppl) (1994) 1991.
[13] E. Sergediene, K. Jonsson, H. Szymusiak, B. Tyrakowska, I.M. Rietjens, N. Cenas, FEBS Lett. 462 (1999) 392.
[14] M. Inoue, N. Sakaguchi, K. Isuzugawa, H. Tani, Y. Ogihara, Biol. Pharm. Bull. 23 (2000) 1153 and references therein.
[15] G. Roy, M. Lombardía, C. Palacios, A. Serrano, C. Cespón, E. Ortega, P. Eiras, S. Lujan, Y. Revilla, P. González-Porqué, Arch. Biochem. Biophys. 383 (2000) 206 and references therein.
[16] T. Gao, Y. Ci, H. Jian, C. An, Vib. Spec. 24 (2000) 225.
[17] C.A. Gomes, T. Girão da Cruz, J.L. Andrade, N. Milhazes, F. Borges, M.P.M. Marques, J. Med. Chem. 46 (2003) 5395 (DOI: http://dx.doi.org/10.1021/jm030956v).
[18] F.A.M. Silva, F. Borges, C. Guimarães, J.L.F.C. Lima, C. Matos, S. Reis, J. Agric. Food Chem. 48 (2000) 2122.
[19] F. Natella, M. Nardini, M. Di Felice, C. Scaccini, J. Agric. Food Chem. 47 (1999) 1453.
[20] K. Tanaka, S. Sakai, S. Tomiyama, T. Nishiyama, F. Yamada, Bull. Chem. Soc. Jpn 64 (1991) 2677.
[21] S. Tomiyama, S. Sakai, T. Nishiyama, F. Yamada, Bull. Chem. Soc. Jpn 66 (1993) 299.
[22] I. Vedernikova, E. Proinov, D.R. Salahub, A. Haemers, Int. J. Quant. Chem. 77 (1999) 161.
[23] P. Rajan, I. Vedernikova, P. Cos, D. Vanden, K. Berghe, A. Augustyns, A. Haemers, Bioorg. Med. Chem. Lett. 11 (2001) 215.
[24] E. Bakalbassis, A. Chatzopoulou, V.S. Melissas, M. Tsimidou, M. Tsolaki, A. Vafiadis, Lipids 36 (2001) 181.
[25] E. van Besien, M.P.M. Marques, J. Mol. Struct. (THEOCHEM) 625 (2003) 265.
[26] M.J. Frisch, G.W. Trucks, H.B. Schlegel, G.E. Scuseria, M.A. Robb, J.R. Cheeseman, V.G. Zakrzewski, J.A. Montgomery Jr., R.E. Stratmann, J.C. Burant, S. Dapprich, J.M. Millam, A.D. Daniels, K.N. Kudin, M.C. Strain, O. Farkas, J. Tomasi, V. Barone, M. Cossi, R. Cammi, B. Mennucci, C. Pomelli, C. Adamo, S. Clifford, J. Ochterski, G.A. Petersson, P.Y. Ayala, Q. Cui, K. Morokuma, D.K. Malick, A.D. Rabuck, K. Raghavachari, J.B. Foresman, J. Cioslowski, J.V. Ortiz, A.G. Baboul, B.B. Stefanov, G. Liu, A. Liashenko, P. Piskorz, I. Komaromi, R. Gomperts, R.L. Martin, D.J. Fox, T. Keith, M.A. Al-Laham, C.Y. Peng, A. Nanayakkara, M. Challacombe, P.M.W. Gill, B. Johnson, W. Chen, M.W. Wong, J.L. Andres, C. Gonzalez, M. Head-Gordon, E.S. Replogle, J.A. Pople, GAUSSIAN 98, Revision A.9, Gaussian Inc., Pittsburgh, PA, USA, 1998.
[27] T.V. Russo, R.L. Martin, P.J. Hay, J. Phys. Chem. 99 (1995) 17085.
[28] A. Ignaczak, J.A.N.F. Gomes, Chem. Phys. Lett. 257 (1996) 609.
[29] F.A. Cotton, X. Feng, J. Am. Chem. Soc. 119 (1997) 7514.
[30] A. Ignaczak, J.A.N.F. Gomes, J. Electroanal. Chem. 420 (1997) 209.
[31] T. Wagener, G. Frenking, Inorg. Chem. 37 (1998) 1805.
[32] F.A. Cotton, X. Feng, J. Am. Chem. Soc. 120 (1998) 3387.
[33] C. Lee, W. Yang, R.G. Parr, Phys. Rev. B37 (1988) 785.
[34] B. Miehlich, A. Savin, H. Stoll, H. Preuss, Chem. Phys. Lett. 157 (1989) 200.
[35] A. Becke, Phys. Rev. A38 (1988) 3098.
[36] A. Becke, J. Chem. Phys. 98 (1993) 5648.
[37] P.C. Hariharan, J.A. Pople, Theor. Chim. Acta 28 (1973) 213.
[38] M.M. Francl, W.J. Pietro, W.J. Hehre, J.S. Binkley, M.S. Gordon, D.J. DeFrees, J.A. Pople, J. Chem. Phys. 77 (1982) 3654.
[39] C. Peng, P.Y. Ayala, H.B. Schlegel, M.J. Frisch, Comp. Chem. 17 (1996) 49.
[40] A.P. Scott, L. Radom, J. Phys. Chem. 100 (1996) 16502.
[41] L. Radom, W.J. Hehre, J.A. Pople, J. Am. Chem. Soc. 94 (1972) 2371.

[42] L.A.E. Batista de CarvalhoT, A.M. Amorim da Costa, J.J.C. Teixeira-Dias, J. Mol. Struct. (Theochem) 205 (1990) 327.
[43] S. García-Granda, G. Beurskens, P.T. Beurskens, T.S.R. Krishna, G.R. Desiraju, Acta Cryst. C43 (1987) 683.
[44] R. Calheiros, N. Milhazes, F. Borges, M.P.M. Marques, J. Mol. Struct. (2004) in press.
[45] N. Karger, A.M. Amorim da Costa, P.J.A. Ribeiro-Claro, J. Phys. Chem. A 103 (1999) 8672.
[46] M.P.M. Marques, A.M. Amorim da Costa, P.J.A. Ribeiro-Claro, J. Phys. Chem. A 105 (2001) 5292.
[47] P. Novak, D. Vikic-Topic, Z. Meic, S. Sekusak, A. Sabljic, J. Mol. Struct. 356 (1995) 131.
[48] S. Sánchez-Cortés, J.V. García-Ramos, Spectrochim. Acta A55 (1999) 2935.
[49] S. Sánchez-Cortés, J.V. García-Ramos, Appl. Spec. 54 (2000) 230.
[50] S. Sánchez-Cortés, J.V. García-Ramos, J. Colloid, Interface Sci. 231 (2000) 98.